

CALCULATION OF ELECTRIC FIELD DISTRIBUTION IN THE VICINITY OF POWER TRANSMISSION LINES WITH TOWERS AND UNMANNED AERIAL VEHICLES PRESENCE

M.M. Rezinkina*, E.I. Sokol, O.G. Gryb, A.V. Bortnikov, S.A. Lytvynenko

National Technical University «Kharkiv Polytechnic Institute»,

Курпичова ст., 2, Kharkiv, 61002, Ukraine,

e-mail: maryna.rezynkina@gmail.com

The results of mathematical modeling of the electric field of overhead power transmission lines (TL) are presented taking into account presence of towers and unmanned aerial vehicles (UAVs) for various cases of the TL lines layout: vertical, horizontal and triangular. Numerical calculations of electric field (EF) were performed using finite integration technique and uniaxial perfectly matched layer. In this case the TL lines under the electrical potential were replaced by linear charges located on their axes. The obtained numerical results for the case of towers and UAV absence were compared with the analytical solutions, which showed coincidence of the EF strength moduli within the range of the assigned accuracy of the numerical calculations— 3%. The results of calculations are necessary to determine the flight height of UAVs, safe from the point of view of electromagnetic compatibility of the on-board electronics to influence of the TL EF and TL towers. References 13, figures 6.

Key words: electric field; mathematical modeling; overhead power transmission lines; electromagnetic compatibility; unmanned aerial vehicles.

Introduction. At present, unmanned aerial vehicles (UAVs) are used to ensure reliable functioning of electric power systems [1,2]. UAVs are used to monitor condition of overhead power transmission lines (TLs) with the help of their optical, thermal and partial discharges recording. There are technical solutions aimed on providing control of UAVs movement by measuring of the magnetic or electric field (EF) strength [3]. The magnetic field strength depends on current and, consequently, on the type of a transmission line electrical load. The parameter independent on such a load is the EF strength; therefore this parameter is most suitable for UAVs navigation.

For reliable functioning of UAV, electromagnetic compatibility of the electronic equipment installed on it with EF of transmission line should be provided. For this it is necessary to investigate power transmission lines EF in the zone above the wires, taking into account the presence of power line towers, as well as conducting elements of UAVs. The results of calculations of power transmission lines EF described in the literature, as a rule, refer to zones located below the power line wires [4]. Information on the EF strength levels above the wires and transmission lines towers is also necessary for estimation of the conditions of corona discharges formation, as well as for choosing the means for their lightning protection. These factors cause the necessity of obtaining information about distributions of the TLs electric field strength.

Calculations of electric and magnetic fields of power transmission lines at presence of such objects as lightning protection cables and cable screens are described elsewhere [4]. Such calculations are carried out mainly with the help of analytical methods [5]. Then it is assumed that the values of potentials, charges and EF strength may be written as complex variables, and their values are calculated using the symbolic method. The electric power transmission line is represented as the sum of EF of its wires and their mirror images relatively the earth's surface [5]. With such a representation of power line for the case of arbitrary wires layout, the capacitance per unit length may be written as [5]

$$C_l = \frac{2\pi\epsilon_m\epsilon_0}{\ln \left[\frac{2 \sqrt[3]{h_1 \cdot h_2 \cdot h_3} \cdot \sqrt[3]{r_{12} \cdot r_{23} \cdot r_{31}}}{r \cdot \sqrt[3]{r'_{12} \cdot r'_{23} \cdot r'_{31}}} \right]}, \quad (1)$$

where h_1, h_2, h_3 are the distances from the earth's surface to each wire; r_{12}, r_{23}, r_{31} are the distances between power line wires; $r'_{12}, r'_{23}, r'_{31}$ are the distances between the wires and their mirror images; r is the radius of power lines wires; ϵ_m is the relative permittivity of the medium with power line wires; $\epsilon_0=0.885 \cdot 10^{-11}$ F/m.

To take into account presence of conducting objects in the vicinity of TL, it is necessary to use numerical methods, for example, the finite integration technique [6]. Such calculations are also necessary for lightning protection means selection [7, 8].

The aim of the paper is to obtain the EF strength distributions over TLs, taking into account distortion of the electric field near TLs' towers and in the vicinity of the conducting parts of UAVs.

Numerical calculation of EF distribution in the vicinity of TLs. The problem of EF calculation in the vicinity of an overhead power transmission line may be considered in quasi-stationary approach. It is assumed that the phases of TL lines potentials (U_1, U_2, U_3) are shifted by an angle 120° and vary by sinusoidal law with 50 Hz frequency. It is assumed also that EF distributions are identical in the cross sections perpendicular to the direction of the lines axes when there are no conducting objects in the TL zone. Calculation of EF strength (\vec{E}) may be carried out with the help of scalar electric potential (ϕ)

$$\vec{E} = -\text{grad} \phi. \quad (2)$$

The source of the TL electric field may be represented as charges distributed with a uniform linear density τ along the lines axes [5]. Complex values of τ may be determined by capacitance of TL per unit length C_l with the help of (1), taking into account the TL lines layout and the diameter of wires $\dot{\tau}_1 = C_l \dot{U}_1$; $\dot{\tau}_2 = C_l \dot{U}_2$; $\dot{\tau}_3 = C_l \dot{U}_3$, where $\dot{U}_1 = Ue^{j0^\circ}$, $\dot{U}_2 = Ue^{j120^\circ}$, $\dot{U}_3 = Ue^{-j120^\circ}$ are the complex line electric potentials; U is the RMS of phase voltage; $j = \sqrt{-1}$.

The equation under consideration is written after application the divergence operator to both sides of the Maxwell equation [9]

$$\text{rot} \vec{H} = \gamma \vec{E} + \frac{\partial \vec{D}}{\partial t} + \vec{J}_{ext}, \quad (3)$$

(where \vec{H} is the magnetic field strength; γ is the specific conductivity; \vec{D} is the electric induction; \vec{J}_{ext} is the current density of external sources) and the integration by the volumes of the elementary cells which cover computational domain. In this case, the continuity equation expressing the law of charge conservation is used [9]

$$\text{div} \vec{J}_{ext} = -\partial \rho_{ext} / \partial t, \quad (4)$$

where ρ_{ext} is the external sources charge density.

By presenting \vec{E} in the form of (2) and applying Gauss's theorem, the final equation written for complex values and derived from (3) and (4) is expressed as

$$\oint_S (-\gamma \cdot \text{grad} \phi - j\omega \epsilon_0 \epsilon \cdot \text{grad} \phi) ds = j\omega \dot{q}_{ext}, \quad (5)$$

where S is the side surface of the cells of computational domain; $\dot{q}_{ext} = \int_V \dot{\rho}_{ext} dV$ is the charge of the external sources, located inside the cell volume V ; ω is the circular frequency.

It is assumed that the charge \dot{q}_{ext} is equal to zero for all cells, except for those through which the TL conductors pass. For cells embracing a wire with potential \dot{U}_1 $\dot{q}_{1ext} = \Delta \cdot C_l \cdot \dot{U}_1$, with potential \dot{U}_2 $\dot{q}_{2ext} = \Delta \cdot C_l \cdot \dot{U}_2$, with potential \dot{U}_3 $\dot{q}_{3ext} = \Delta \cdot C_l \cdot \dot{U}_3$ (where Δ is the cell length in the direction of the current conductor, C_l is calculated in accordance with (1)).

The operations of differentiation are replaced by their difference analogues at numerical realization of (5). This approach, when the law of conservation (in this case the law of charge conservation) is used to obtain a numerical solution, is referred as the finite integration technique [10]. The advantage of the finite integration technique consists in the automatic fulfillment of boundary conditions on the media interfaces.

At numerical calculations of TLs EF using finite-difference methods, the problem owing to power lines location in so-called open regions arises. The dimensions of the calculation domain at the outer boundaries with assigned zero conditions for EF strength are very large. To solve this problem, UPML (uniaxial perfectly matched layers) are used [11]. It is assumed that anisotropic layers are located at the boundaries of the calculation domain, the electrical parameters of which (relative permittivity ϵ in our case) are proportional to some value a ($a > 0$) in the direction parallel to the external boundary of the calculation domain, and ϵ is proportional to $1/a$ in the direction perpendicular to the external boundary of the calculation domain. The value of ϵ changes by exponential law in each layer, and the values of a increase near the outer boundary of the calculation domain. For example, for the layer parallel to the plane x - y , the relative dielectric permittivity tensor is expressed as

$$\bar{\varepsilon}_z = \begin{bmatrix} a_z & 0 & 0 \\ 0 & a_z & 0 \\ 0 & 0 & a_z^{-1} \end{bmatrix}.$$

At the *UPML* intersection in the corners of the computation domain, the tensors of intersecting layers are

multiplied

$$\bar{\varepsilon} = \begin{bmatrix} a_x^{-1} & 0 & 0 \\ 0 & a_x & 0 \\ 0 & 0 & a_x \end{bmatrix} \cdot \begin{bmatrix} a_y & 0 & 0 \\ 0 & a_y^{-1} & 0 \\ 0 & 0 & a_y \end{bmatrix} \cdot \begin{bmatrix} a_z & 0 & 0 \\ 0 & a_z & 0 \\ 0 & 0 & a_z^{-1} \end{bmatrix},$$

where $a_x(x)=1+(k_{max}-1)(x/d)^m$; $a_y(y)=1+(k_{max}-1)(y/d)^m$; $a_z(z)=1+(k_{max}-1)(z/d)^m$; d is the thickness of *UPML*; $k_{max}=300-500$ and $m=3-5$ are the factors [11].

To calculate the EF, the Cartesian coordinate system is used. It is assumed that the wires of the transmission lines are parallel to axis *Oz*, axis *Oy* is perpendicular to the earth's surface, and axis *Ox* is perpendicular to the transmission lines direction and parallel to the earth's surface. The coordinate system zero point is assumed to be located on the earth surface.

Taking into account that (1) contains the relative permittivity of the medium in *UPML* zones with the transmission lines wires directed along the axis *Oz*, the value of ε_m is set to be equal to $\varepsilon_m=\varepsilon_x$ or $\varepsilon_m=\varepsilon_y$.

Calculations of power transmission lines EF for their different locations. Software that realizes the described numerical method was developed using Fortran programming language. EF calculations were performed for TL of 220 kV RMS linear voltage. Then $U = 220 \cdot 10^3 / \sqrt{3}$ V, the distance between the TL lines is not less than 6 m, the length of the insulator on which a wire is suspended from a TL tower is equal to 0.8 m, layouts of the TL lines are triangular, horizontal or vertical [12]. For calculation with the help of the finite integration technique, a rectangular grid with a step Δ was applied to the calculation domain. Dimensions of the domain are $x_{min}, x_{max}, y_{min}=0, y_{max}, z_{min}=0, z_{max}$. *UPML* are located at the boundaries of the calculation domain. *UPML* parameters are follows: the number of layers is equal to 10, $k_{max}=300$, $m=3$. In the numerical calculations, the following boundary conditions are used: $\partial\phi/\partial x = 0$ at $x=x_{min}, x=x_{max}$; $\phi = 0$ at $y=y_{min}=0$, $\partial\phi/\partial y = 0$ at $y=y_{max}$; $\partial\phi/\partial z = 0$ at $z=z_{min}=0, z=z_{max}$. It was taken into account that due to *UPML* application, the values of the EF strength in the corresponding directions at $x=x_{min}, x=x_{max}, y=y_{max}, z=z_{max}$ can be assigned equal to zero. A condition $\phi = 0$ at $y=y_{min}=0$ takes into account presence of the earth with zero potential. As an assumption, condition $\partial\phi/\partial z = 0$ at $z=z_{min}=0$ is accepted, as it is assumed at this problem solution that the TL lines are infinitely long and parallel to the surface of the earth. The earth is represented as a conducting infinite half-space. Such conditions are usually accepted at the EF of transmission lines calculation [4, 5]. The influence of the TL wires sagging and ground surface irregularities on the EF of transmission lines distribution is not considered in this paper. In the case of a conductive object presence near a TL, which distorts its EF distribution, it was assumed that the *Oz* axis passes through its axis of symmetry.

Usage of the finite integration technique allows application of a relatively large spatial step along axes *Ox, Oy, Oz*: $\Delta_x=\Delta_y=\Delta_z=\Delta=0.4$ m. The carried numerical experiments, which consisted in double increase of the computation domain dimensions and a double decrease of the spatial grid step, have shown that further decrease of the spatial step and increase of the computation domain dimensions do not cause changes in the EF distributions. Dimensions of the calculation domain in the direction of the axes *Ox, Oy, Oz* are shown in Figs. 1–3, 6.

Calculations of the EF distributions for various TL-220 lines layouts: triangular, horizontal and vertical were carried out. Comparison of the EF distributions obtained with the help of numerical calculations and analytical solutions [5, 13] for three types of TL lines layout in absence of TL towers and UAVs has shown coincidence of the EF strength values within the assigned at numerical calculations relative error – 3 %. Fig. 1, *a* shows the results of numerical (solid curves) and analytical calculations (dashed curves) of the distributions of lines of equal EF strength (in V/m), proving their good coincidence. The lines of equal potentials, EF strength and other dependencies were got with the help of standard programs.

Pictures of the EF distributions for TL-220, calculated with the help of the described approach, are shown in Figs. 1–3, 6. The following designations are used: 1 is the earth, 2 are the TL lines, 3 is the TL tower, 4 are *UPML*, 5 is the UAV.

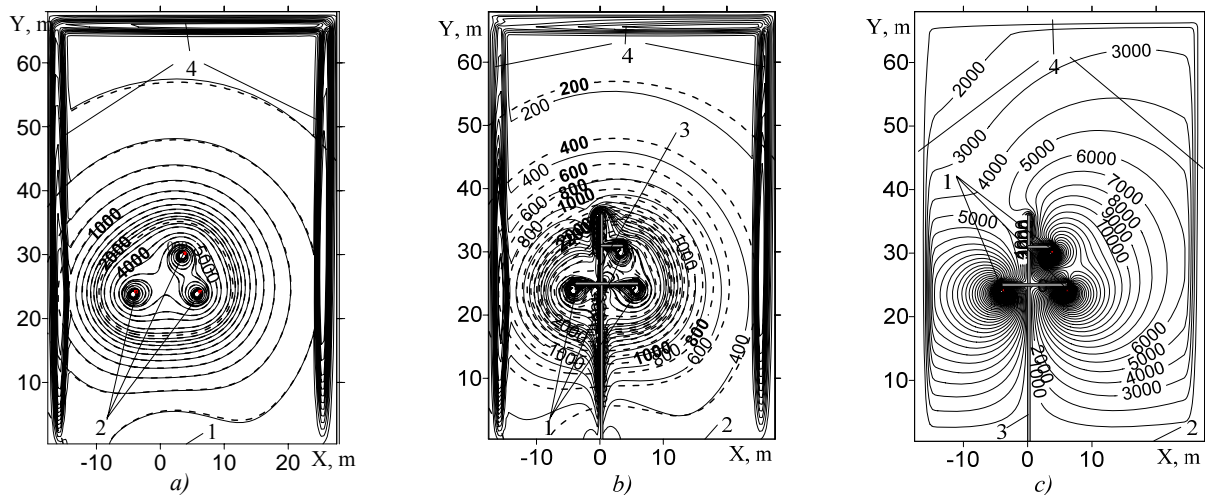


Fig. 1

The analytical solutions for the cases for any objects absence in the TL zone are shown in Fig. 1–3 by the dashed lines. These figures show calculated distributions of lines of equal EF strength (Fig. 1, *a, b*, 2, 3, 6, data are given in V/m) as well as the lines of equal potential (Fig. 1, *c*, data are given in V) in the sections perpendicular to the TL lines ($z=0$) in the entire calculation domain, including UPML. The results of calculations performed taking into account presence of a TL tower are shown in Fig. 1, *b, c*, 2, 3 in the cross-sections passing through its middle.

The height of the TL tower and the maximum height of TL lines suspension are assigned equal to 36 m and 30 m correspondingly. Fig. 1 represent the case of a triangle lines layout; distributions shown in Fig. 1, *a* are calculated for the case of any objects absence of in the TL zone.

Fig. 2 shows the computed distributions of the lines of equal EF strength for the case of a horizontal (*a*) and a vertical (*b*) layout of the TL lines in TL towers presence. The calculated EF distribution for TL towers absence is shown in Fig. 2, *a* by the dotted lines.

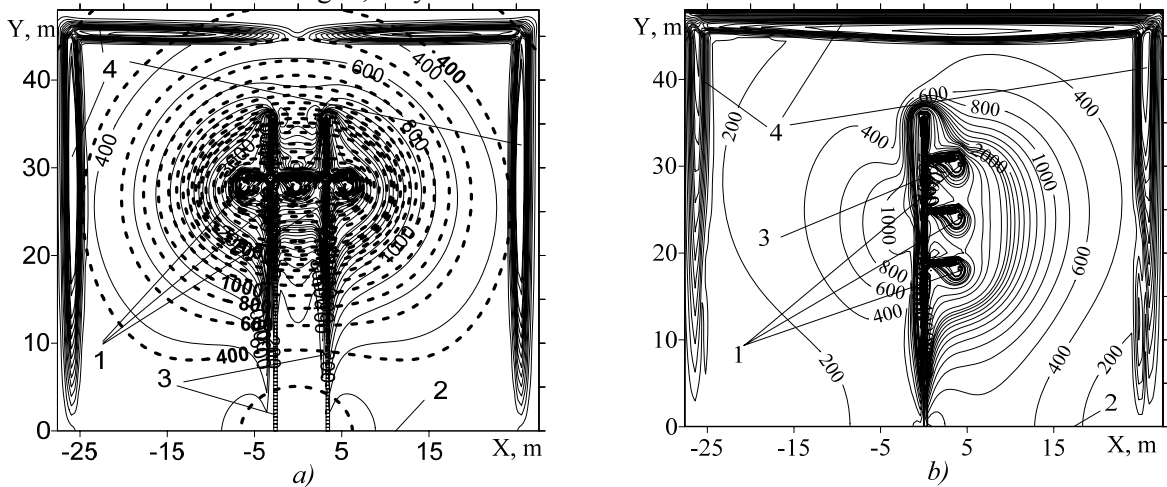


Fig. 2

To simplify the EF calculation with regard of a TL tower presence, it was represented schematically as having a constant cross section along its entire height, which is equal to 0.4×0.4 m. In order to estimate the effect of a real TL tower narrowing to the top, calculations of the EF were carried with such its representation.

Fig. 3, *a* shows the calculated distributions of lines of equal EF strength in the cross-section $z=0$ for this case (solid lines) and also the distribution for the case of a tower with a constant cross-section along its height (dashed lines) when the TL lines layout is a triangle. As can be seen from this figure, a character of the TL tower representation has not significant influence on the EF distribution in the zone above the tower. Fig. 3, *b* shows calculated results of the EF strength (in V/m) for this geometry in the cross-section $x = 0$. This cross-section passes through the middle of the tower and the TL lines do not get into it (their projections on this cross-section are marked by callout 1).

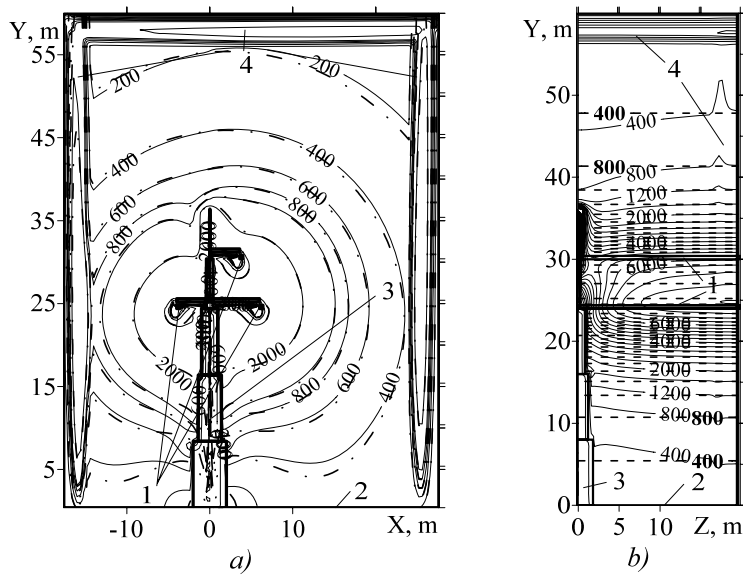


Fig. 3

decreases faster than in the case of its absence.

Fig. 4 shows calculated dependences of the maximum EF strength levels over the TL lines for different cases of their layout: triangular (marked \bullet), horizontal (marked \circ) and vertical (marked $+$).

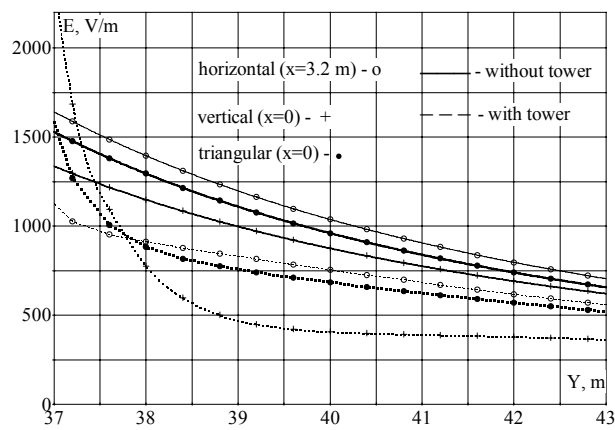


Fig. 4

These distributions show differences in the EF strength in the same areas for the cases of absence (solid lines) or presence (dashed lines) of the TL towers. These curves correspond to the points on a straight line perpendicular to the earth surface, where the distortion of the EF because of the TL tower presence is maximal. This line is located 1 m and more above the TL tower. These maximum levels are reached at different magnitudes of the coordinate x shown in the figure. It follows from the dependencies of Fig. 4 that increase in the EF strength because of a TL conductive grounded tower presence, which takes out a zero potential to its vertex, extends only in a relatively small zone (about 2–3 m for the considered TL configurations) directly above the vertex of tower, and the EF strength decreases above this height in comparison with the case of a tower absence. It may be seen from the comparison of the solid and dashed lines in Fig. 4. As can be seen from this figure, for the considered zones, the highest levels of the EF strength occurs when the TL lines have a horizontal layout. Maximum levels of the EF strength with a vertical TL lines layout are achieved not above a TL tower, but above the TL lines.

Fig. 5 shows the calculated levels of maximum EF strength above the TL lines in the zone where there are no towers for a triangular (1), horizontal (2) and vertical (3) TL lines layout. These dependencies on the vertical coordinate y are plotted in the cross-section $z=\text{const}$ for different values of x corresponding to the zones with maximum levels of the EF strength for the height $y>35$ m: curve 1 and 2 – for $x=0$, curve 3 – for $x=4$ m.

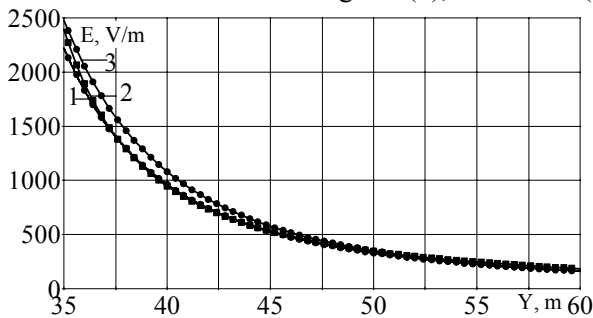


Fig. 5

As can be seen from Fig. 5, the highest levels of the EF strength occur when the TL lines layout is horizontal, but for $y>55$ m the differences in the EF strengths for all three cases of the TL lines layout are negligible.

The dashed and dot lines in Fig. 3, *b* show the results of the analytical solution. It is follow from Fig. 3, *b*, that the EF distortion due to a TL tower presence is observed in a relatively small zone (5–10 m), detached from the tower in the direction of the TL lines, mostly near the top and the base of the tower.

As follows from analysis of the calculated EF of transmission lines, at the TL towers presence (see Figs. 1–3), the magnitude of the EF strength in a relatively small zone just around the tower vertice increases for the considered cases by a factor 2–8 compared with the EF strength at their absence. However, the EF strength in the area further above the TL tower

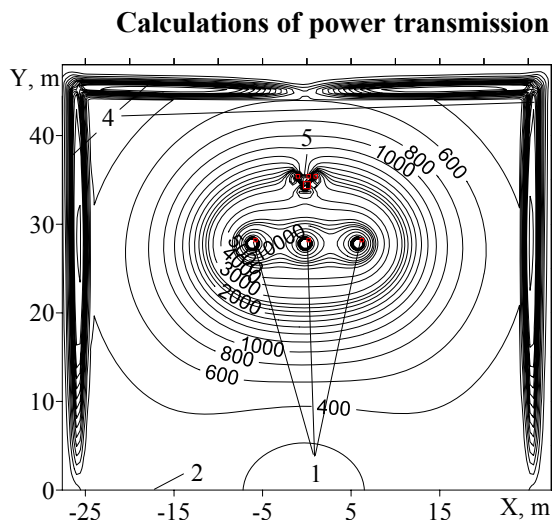


Fig. 6

Calculations of power transmission lines EF at an UAV presence. Usually some parts of UAVs are made of conductive materials. For instance, batteries and motors of UAVs as a rule are conductive. UAVs location over TLs causes the EF distortion and appearance of the zones with increased EF strength levels compared with the case of their absence. Information on the levels of the EF strength inside UAVs, taking into account such amplification, is necessary for choosing the type of electronic equipment, as well as making decisions on its shielding, if necessary. Fig. 6 shows the calculated distributions of lines of equal EF strength (in kV/m) in an UAV presence in the cross-section $z=0$, passing through its center, for the case of TL-220 lines horizontal layout. As follows from the calculations, increase in the EF strength around the conducting parts of UAV for the considered model can reach about 3 times in comparison with the case of the UAV absence.

Conclusions. 1. As shown by numerical

experiments, the zones with the highest EF strength levels are observed over TLs with a horizontal layout, but differences of EF strength of TL-220 with horizontal, vertical and triangular layouts are negligible at distances above the lines exceeding 15 m.

2. Calculations of the EF, performed taking into account presence of TL towers, have shown that the EF strength increases in the zone located 1–2 m above a tower. When this height is exceeded, the EF strength just above a tower decreases and becomes less than the EF strength for the case of a tower absence. Obtained results of calculations of the EF strength distribution allow determining the zones of safe functioning of the electronic components of UAVs and, if necessary, to take measures to ensure their shielding. Such calculations are also necessary to assess the conditions for corona formation on power lines and choose the means for their lightning protection.

1. Arbuzov R.S., Ovsyannikov A.G. Modern methods of diagnostics of overhead power lines. Novosibirsk: Nauka, 2009. 136 p. (Rus)

2. Skarbek L., Zak A., Ambroziak D. Damage detection strategies in structural health monitoring of overhead power transmission system. 7th European Workshop on *Structural Health Monitoring*, July 8-11, 2014. La Cité, Nantes, France. Pp. 663 – 670.

3. Kachesov V.E., Lebedev D.E. Air diagnostic method of high voltage transmission lines. Patent Russian Federation. No 2483314. 2013. (Rus)

4. Dikoy V.P., Tokarskiy A.Yu., Rubcova N.B., Krasin O.V. Cable screens and their usage on the 500 kV overhead transmission lines. Increasing the efficiency of power systems. Iss. 4. Moskva: Energoatomizdat, 2001. Pp. 209 – 215. (Rus)

5. Demirchyan K.S., Neiman L.R., Korovkin N.V., Chechurin V.L. Theoretical foundations of electrical engineering. Vol. 3. Moskva: Piter, 2006. 377 p. (Rus)

6. Rezinkina M.M., Rezinkin O.L. Calculation of 3-D electrical field intensity distribution in heterogeneous dielectric. *Elektrichestvo*. 1995. No 7. Pp. 62-66.

7. Rezinkina M.M. Technique for predicting the number of lightning strokes to extended objects. *Technical Physics*. 2008. Vol. 53. No 5. Pp. 533-539.

8. Rezinkina, M.M., Knyazyev, V.V., Kravchenko, V.I. Mathematical description of leader channel propagation for selection of model experiment parameters and lightning guard systems. *Technical Physics*. 2007. Vol. 52. No 8. Pp. 1006 – 1010.

9. Tamm I.E. Fundamentals of the theory of electricity. Moskva: Nauka, 1989. 504 p. (Rus)

10. Patankar S. Numerical methods for solving problems of heat transfer and fluid dynamics. Moskva: Energoatomizdat, 1984. 150 p. (Rus)

11. Taflove A., Hagness S. Computational electromagnetics: the finite difference time domain method. Boston-London: Artech House, 2000.

12. Rules for the installation of electrical facilities. Kharkiv: Fort, 2017. 760 p. (Ukr)

13. Sokol E.I., Rezinkina M.M., Grib O.G., Vasilchenko V.I., Zuev A.A., Bortnikov A.V., Sosina E.V. Technique of complex automated monitoring of the Ukraine energy system objects aiming on increase of its operation safety. *Electrical Engineering & Electromechanics*. 2016. No 2. Pp. 65-70. (Rus)

РОЗРАХУНОК РОЗПОДІЛУ ЕЛЕКТРИЧНОГО ПОЛЯ В ОКОЛИЦІ ЛІНІЙ ЕЛЕКТРОПЕРЕДАЧІ З УРАХУВАННЯМ НАЯВНОСТІ ОПОР І БЕЗПЛОТНИХ ЛІТАЛЬНИХ АПАРАТІВ

М.М. Резинкіна, Є.І. Сокол, О.Г. Гриб, О.В. Бортніков, С.А. Литвиненко

Національний технічний університет «Харківський політехнічний інститут»,

вул. Кирпичова, 2, Харків, 61002, Україна,

e-mail: marvna.rezvnkina@gmail.com

Представлено результати математичного моделювання електричного поля повітряних ліній електропередачі (ЛЕП) з урахуванням наявності опор і безпілотних літальних апаратів (БПЛА) для різних випадків розташування проводів ЛЕП: вертикального, горизонтального і трикутного. Чисельні розрахунки електричного поля (ЕП) виконувалися за допомогою методу кінцевого інтегрування і одночасно добре узгоджених шарів. При цьому струмопроводи, що знаходяться під потенціалом, замінювалися лінійними зарядами, розташованими на їхніх осях. Виконано порівняння отриманих чисельних результатів для випадку відсутності опор і БПЛА з аналітичними рішеннями, яке показало збіг модулів напруженості ЕП у межах заданої точності чисельних розрахунків – 3%. Результати розрахунків необхідні для визначення висоти польоту безпілотних літальних апаратів, безпечної з точки зору електромагнітної сумісності бортової електроніки до дії ЕП ЛЕП та їхніх опор. Бібл. 13, рис. 6.

Ключові слова: електричне поле; математичне моделювання; повітряні лінії електропередачі; електромагнітна сумісність; безпілотні літальні апарати.

УДК 621.316.98

РАСЧЕТ РАСПРЕДЕЛЕНИЯ ЭЛЕКТРИЧЕСКОГО ПОЛЯ В ОКРЕСТНОСТИ ЛИНИЙ ЭЛЕКТРОПЕРЕДАЧИ С УЧЕТОМ НАЛИЧИЯ ОПОР И БЕСПИЛОТНЫХ ЛЕТАТЕЛЬНЫХ АППАРАТОВ

М.М. Резинкина, Е.И. Сокол, О.Г. Гриб, А.В. Бортников, С.А. Литвиненко

Национальный технический университет «Харьковский политехнический институт»,

ул. Кирпичева, 2, Харьков, 61002, Украина,

e-mail: marvna.rezvnkina@gmail.com

Представлены результаты математического моделирования электрического поля воздушных линий электропередачи (ЛЭП) с учетом наличия опор и беспилотных летательных аппаратов (БПЛА) для различных случаев расположения проводов ЛЭП: вертикального, горизонтального и треугольного. Численные расчеты электрического поля (ЭП) выполнялись с помощью метода конечного интегрирования и одноосно хорошо согласованных слоев. При этом находящиеся под потенциалом токопроводы заменялись линейными зарядами, расположенными на их осях. Выполнено сравнение полученных численных результатов для случая отсутствия опор и БПЛА с аналитическими решениями, показавшее совпадение модулей напряженностей ЭП в пределах заданной точности численных расчетов – 3%. Результаты расчетов необходимы для определения высоты полета беспилотных летательных аппаратов, безопасной с точки зрения электромагнитной совместимости бортовой электроники к действию ЭП ЛЭП и их опор. Библ. 13, рис. 6.

Ключевые слова: электрическое поле, математическое моделирование, воздушные линии электропередачи, электромагнитная совместимость, беспилотные летательные аппараты.

1. Арбузов Р.С., Овсянников А.Г. Современные методы диагностики воздушных линий электропередачи. Новосибирск: Наука, 2009. 136 с.
2. Skarbek L., Zak A., Ambroziak D. Damage detection strategies in structural health monitoring of overhead power transmission system. 7th European Workshop on *Structural Health Monitoring*, July 8-11, 2014. La Cité, Nantes, France. Pp. 663 – 670.
3. Качесов В.Е., Лебедев Д.Е. Способ аэродиagnостики высоковольтной линии электропередачи. Патент РФ № 2483314. 2013.
4. Дикой В.П., Токарский А.Ю., Рубцова Н.Б., Красин О.В. Тросовые экраны и их применение на ВЛ-500 кВ. Тр. ИГЭУ. Повышение эффективности работы энергосистем. Вып. 4. М.: Энергоатомиздат, 2001. С. 209-215.
5. Демирчян К.С., Нейман Л. Р., Коровкин Н.В., Чечурин В.Л. Теоретические основы электротехники. Том 3. М.: Питер, 2006. 377 с.
6. Rezinkina M.M., Rezinkin O.L. Calculation of 3-D electrical field intensity distribution in heterogeneous dielectric. *Elektrichestvo*. 1995. No 7. Pp. 62-66.
7. Rezinkina M.M. Technique for predicting the number of lightning strokes to extended objects. *Technical Physics*. 2008. Vol. 53. No 5. Pp. 533-539.
8. Rezinkina, M.M., Knyazyev, V.V., Kravchenko, V.I. Mathematical description of leader channel propagation for selection of model experiment parameters and lightning guard systems. *Technical Physics*. 2007. Vol. 52. No 8. Pp. 1006 – 1010.
9. Тамм И.Е. Основы теории электричества. Москва: Наука, 1989. 504 р.
10. Патанкар С. Численные методы решения задач теплообмена и гидродинамики. Москва: Энергоатомиздат, 1984. 150 р. (Rus)
11. Taflove A., Hagness S. Computational electromagnetics: the finite difference time domain method. Boston-London: Artech House, 2000.
12. Правила улаштування електроустановок. Харків: Форт, 2017. 760 с.
13. Сокол Е.И., Резинкина М.М., Гриб О.Г., Васильченко В.И., Зуев А.А., Бортников А.В., Сосина Е.В. Методика комплексного автоматизированного мониторинга объектов энергетической системы Украины с целью повышения безопасности ее функционирования. *Електротехніка і Електромеханіка*. 2016. № 2. С. 65-70.

Надійшла 18.09.2017
Остаточний варіант 19.10.2017